Kinematics Modelling of Sit-to-Stand Exercise for the Lower Extremities Rehabilitation

Piotr Falkowski, Jan Oleksiuk, and Kajetan Jeznach

Abstract This paper presents a kinematic modelling approach for sit-to-stand (STS) exercises performed with a lower extremity rehabilitation exoskeleton integrated with a mobile platform and lifting column. Experimental joint and pelvis kinematics were acquired using an IMU-based motion capture system across three STS variants that differed in their upper-limb support strategies. Measured joint trajectories were used to compute the required platform translation trajectories within the motion, as well as the needed column stroke, and the passive compensation ranges along all compliant axes. Results show that hip and knee flexionextension dominate within STS, while pelvic lateral translation and anterior tilt generate the largest compensation demands, typically ranging to approximately 17 mm and 6ř, respectively. The analysis indicates that the mobile platform displacement is no larger than 800 mm, and the maximum lifting column stroke is approximately 860 mm for the considered STS executions. The proposed modelling framework and dataset provide a basis for designing passive and active compensation mechanisms, mobile platform driving systems, lifting columns, and predictive control algorithms for mobile rehabilitation exoskeletons performing task-oriented STS training.

P. Falkowski
Łukasiewicz Research Network - Industrial Research Institute for Automation and Measurements PIAP, Warsaw, Poland
e-mail: piotr.falkowski@piap.lukasiewicz.gov.pl

J. Oleksiuk
Łukasiewicz Research Network - Industrial Research Institute for Automation and Measurements PIAP, Warsaw, Poland

K. Jeznach
Łukasiewicz Research Network - Industrial Research Institute for Automation and Measurements PIAP, Warsaw, Poland

1 Introduction

The sit-to-stand (STS) motion is a critical functional movement integral to independent living [4]. Therefore, it is commonly used in task-oriented physiotherapy and as part of gait reeducation. It encompasses a complex coordination of the lower extremity full kinematic chain and pelvic joints [2]. It is also used as a clinical marker of mobility and fall risk, particularly among elderly and neurologically impaired populations [7]. As the STS is relatively physically demanding for a physiotherapist or multiple therapists to support, the robotization of such treatment has been widely investigated in recent years [8].

Because the STS involves the entire lower extremity kinematic chain, it is most effective to use exoskeleton-type rehabilitation robots to support the exercise. Such devices need to actuate or enable passive motion of at least hip, knee, and ankle flexion/extension [10]. However, designs often incorporate more degrees of freedom (DOFs) to better mimic the natural biomechanics of STS movement. Investigation into the actuation and control of such systems reveals the need for robust solutions that accommodate individual user variability and support smooth transition trajectories [11]. Even though contemporary systems for active treatment employ advanced strategies to incorporate users' intentions, based on forces or even biomedical signals, into the control loop [3].

The hip joints complex motion necessitates advanced biomechanical modeling to replicate its crucial role in STS motion. Recent studies emphasize the functional benefits of adding additional DOFs to the hip in exoskeleton designs, enabling more physiologically accurate movements and improved balance during standing up [14, 4, 5]. These include abduction/adduction and internal/external rotations. Besides, the asymmetrical activity of the two extremities and involved non-modeled mobility (e.g., metatarsophalangeal joint) can result in inaccuracies in computing motion of characteristic points (e.g., motion of the modeled hip central point regarding the floor) or additional tilt of the pelvis [1].

Advanced exoskeletons now aim to simulate complex pelvic kinematics, integrating lateral and anterior-posterior pelvic shifts critical for maintaining the center of mass within the base of support during STS [9]. These developments are particularly beneficial for patients with neurological conditions who struggle with symmetrical, controlled pelvic movements.

Most lower-extremity exoskeletons are wearable devices used independently in gait treatment [5]. However, they require additional tools for supporting balance, such as crouches or constant physical support from a physiotherapist [8]. On the contrary, there are designs integrated with either mobile platforms that support the balance of the device and enable real mobility , or exoskeletons with a suspension system that enable simulated gait exercise while stationary above ground, optionally integrated with treadmills [6]. Both approaches significantly reduce fall risk. Nevertheless, the paper focuses on the former method, as it enables a broader range of therapeutic exercises in real-world scenarios that include STS.

An exoskeleton attached to the mobile platform, however, becomes a closed kinematic chain. Both the platform and at least one foot sole remain in contact with the ground [12]. Therefore, the kinematics of the mobilized extremity joints and the transitional movement of the platform, and, if used, the lifting column, need to be synchronized. Moreover, mobility not accounted for in kinematic computations for the control algorithm can result in inaccuracies that must be compensated for mechanically in the system. This can be realized with compliant mechanisms, backlash, or backdriveability of selected motors [13].

The recent literature demonstrates continuous progress in modeling sit-to-stand biomechanics and applying these models to robotic exoskeleton designs for rehabilitation. Systems integrated with mobile platforms enable effective, minimally supervised therapy in real-life scenarios. However, they require much more complex kinematic models to guarantee ergonomics, remain in contact with the floor, and execute genuine pelvis motion in STS. This paper aims to fill a scientific gap in this area, develop kinematic models for STS supported by exoskeletons with a mobile platform, and define the real-life compensation mechanisms required by the system.

2 Methodology

For modeling the device, a universal structure consisting of a driven mobile platform with a driven lifting column was assumed. Its general structure is presented in Fig. 1. Each exoskeleton's extremity frame independently supports the hip's three DOFs, and flexion/extension of the knee and ankle joints (represented by φ joint variables). The exoskeleton is attached to the lifting column via the compliant system, which can compensate transitional and rotational inaccuracies along all main axes of its local frame of reference ($\mathrm{x_c}$, $\mathrm{y_c}$, and $\mathrm{z_c}$,). It is assumed that during STS motion, the platform is moving only along the x-axis of the global frame of reference (represented by the x_1 variable). This frame of reference is set in the platform's front wheel bottom at the beginning of the modeled motion. The lifting column can extend only vertically (represented by the x_2 variable). Point **G** indicated in Fig. 1 is a modelled most posterior point of constant contact of the exoskeleton with the ground during the STS exercise. However, the foot sole support of the system, which includes **G** point, is flexible, which is not considered in the furtherly developed kinematics formulas.

Theoretical equation for computing kinematics of **G** point in global frame of reference for the left leg is presented in formula 1. In the formula, symbols $\boldsymbol{r}_j^{(i)}$ represent vectors between the centers of frames of reference assigned

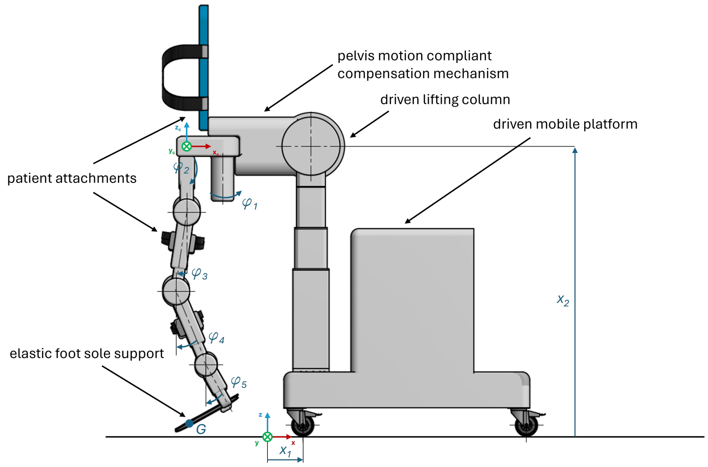

Fig. 1 Description of the device's kinematics (x - driven translational parameters, φ - driven rotational joint parameters) and critical components of the system (left side)

to the i-th and j-th rotations in the frame of reference assigned to the i-th rotation.

$$\begin{aligned} \boldsymbol{r}_G^{(0)} = \quad & \boldsymbol{r}_1^{(0)} + \boldsymbol{R_y}(\varphi_1)\left(\boldsymbol{r}_2^{(1)} + \boldsymbol{R_x}(\varphi_2)\left(\boldsymbol{r}_3^{(2)} + \boldsymbol{R_y}(\varphi_3)\left(\boldsymbol{r}_4^{(3)} + ...\right.\right.\right. \\ & \left.\left.\left. + \boldsymbol{R_y}(\varphi_4) \cdot \left(\boldsymbol{r}_5^{(4)} + \boldsymbol{R_y}(\varphi_4) \cdot \boldsymbol{r}_G^{(5)}\right)\right)\right)\right) \end{aligned} \tag{1}$$

Compensations in the compliant mechanisms are computed based on the differences between the x_1 and x_2 parameters for the left and right extremities, as well as on the differences between their values computed using the kinematics formulas and those measured by the motion capture system independently. These will be described by a compensation vector regarding the axes of a frame of reference presented in Fig. 1.

To model the motion, the *Noraxon MR4* environment with seven *Noraxon Ultium Motion* IMU sensors and two 2D *Noraxon NiNOX 120* cameras facing the front and left side of a participant was used. IMU sensors were attached according to the standard positioning in *Noraxon* documentation at feet, shanks, thighs, and pelvis (lower sensor placement). The motion was recorded repeatedly in three variants, with five repetitions each, by independent volunteers of different genders aged 23-64. The volunteers' heights ranged from 166 cm to 190 cm. The variants varied in terms of possible hand support: front pulling the rack (variant 1), back-of-seat push (variant 2), or no support possible (variant 3). The height of the chair used for the experiment was 44 cm.

Motion capture included tracking of flexion-extension angles in the knee and ankle, as well as full anatomical angles of the hip joints. Additionally, the translational motion of both hips' modelled centres was tracked. The measurements were performed simultaneously for both extremities. The measured trajectories served as inputs for kinematic simulations and further analysis.

For comparison purposes, each repetition was normalized in terms of time to match the nominal length of the repetition in a certain variant.

3 Results and discussion

Joint kinematics of the exoskeleton were computed based on the extremity joint kinematics registered with the *Noraxon* system. Their plots for three variants are presented in Fig. 2. The most active motions include hip and knee flexion/extension (φ_3 and φ_4). Ankle flexion/extension (joint 5) is used with a much lower range and acts mostly upon flexion.

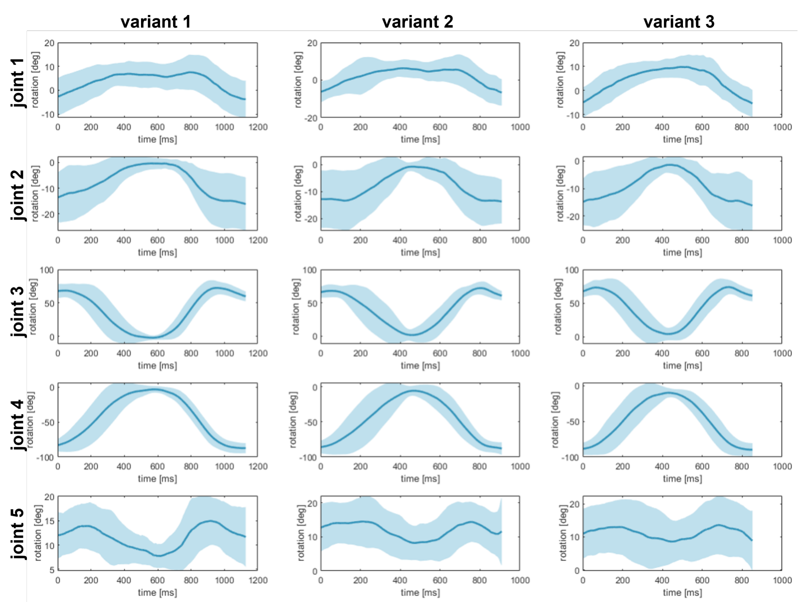

Fig. 2 Exoskeleton's joint kinematics for three different variants of exercise (mean and standard deviation presented; all participants' left extremities)

However, also internal and external rotations were engaged in the range of -10 to +15 degrees and differed significantly between individual participants. This motion requires active support from the first exoskeleton joint. Moreover, due to asymmetrical motion regarding the sagittal plane, hip adduction/abduction was also engaged, reaching up to 20 degrees typically from low negative values. This resulted in the required motion of the second exoskeleton rotational joint. Such a motion may also result in lateral pelvic motion during STS exercise.

It can be observed that the variants do not affect significantly the average joint trajectories. Nevertheless, no support (variant 3) results in much greater variability in ankle flexion/extension, due to the need to balance. Moreover, unsupported motions are also shorter and more dynamic for the same reason.

Pelvis motion was computed using kinematic formulas and compared with motion tracked using video-based motion capture. The ranges of the components of $\boldsymbol{T}_c^{(0)}$ are represented in Fig. 3. The compensations are presented as the absolute values, and it is assumed that the motions can be fully symmetrical.

It is notable that the biggest compensations are correlated to the lateral pelvis motions (T_y) and its anterior tilt (T_{α_y}). The majority of the former remains within the range of ± 6 degrees, while the latter remains within the range of ± 17 mm. However, outliers up to ± 7 degrees and ± 55 mm are observed. The remaining angular compensations are limited to ± 3 degrees with outliers reaching the maximum of ± 4.5 degrees. For the transitional compensations, the majority of anterior/posterior and inferior/superior compensations remain in the range of ± 8 mm, with outliers reaching the maximum of ± 13 degrees.

A clear trend of increased compensation related to the y-axis for chair back support (variant 2) can be observed. It relates to the need to reach back with the pelvis bent and to the relative lateral motion of the pelvis during spine rotation.

The mobile platform is expected to move in both front-to-rear and rear-to-front directions, while the lifting column is expected to move either up or down during sit-to-stand exercises. The presented kinematic formulas enable the computation of required movements from joint measurements. Joint trajectories measured for three different exercise variants were used to compute the transitional trajectories' displacements of the mobile platform (x_1) and the lifting column (x_2). These, referred to the base state upon sitting position, are presented in Fig. 4.

In general, the variants do not strongly affect the shapes of the required trajectories for platform and column motions. However, no-support attempts result in wider variability between individuals' repetitions. Based on the analysis results, during the STS exercise, the mobile platform is expected to move no more than 800 mm, while the column stroke of operation is estimated at 860 mm.

4 Summary

The conducted experiments resulted in the construction of kinematics models enabling the analyzed exoskeleton, based on a mobile platform, to reproduce

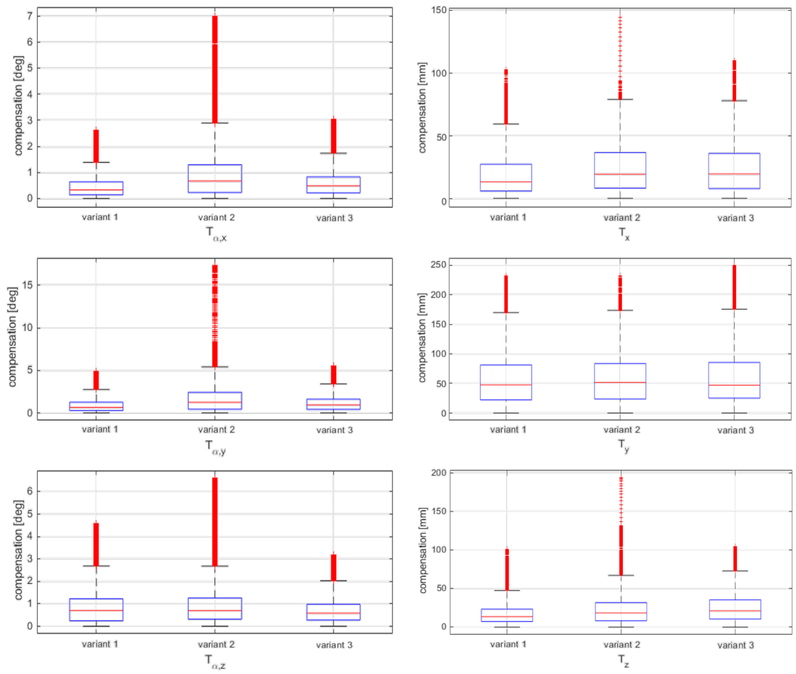

Fig. 3 Ranges of compensation vectors' components required all participants; different variants distinguished (absolute values)

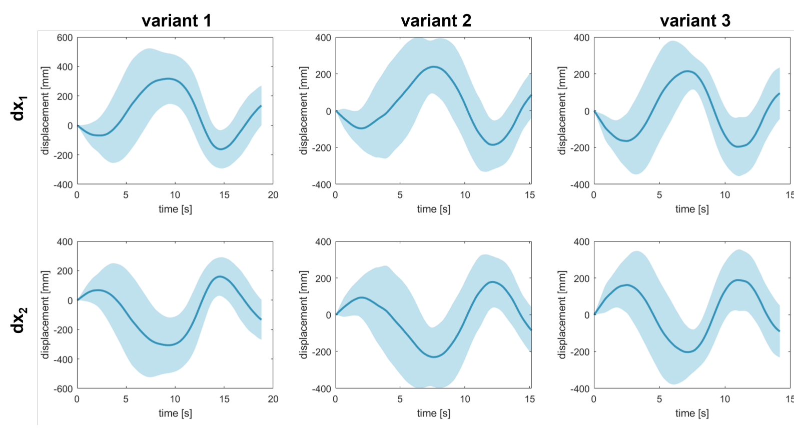

Fig. 4 Transitional motions of mobile platform and lifting column needed for three different variants of exercise (mean and standard deviation; all participants)

functional sit-to-stand motion using a closed-chain structure. The derived equations enable direct computation of these trajectories from measured joint angles, facilitating control over STS task-oriented exercising.

The compensation analysis demonstrates that relatively small, but non-negligible, pelvic translations and rotations must be accommodated by compliant mechanisms to preserve realistic STS patterns. These results will serve as a basis for designing a compliant mechanism for similar structures.

Experimental results show that the three investigated STS variants exhibit similar joint ranges but differ in compensation, as well as in the motions of the lifting column and mobile platform. Computed ranges for the analyzed variables enable the design of a mobile platform while selecting appropriate driving mechanisms and a lifting column with a sufficient stroke and vertical speed.

The investigation provides insight into STS kinematics, which are critical for treatment. A similar approach can be used to model other task-oriented exercises for the lower extremities and validate whether they can be performed with the proposed setup. Moreover, the approach can be transferred to other designs by modifying the kinematic formulas. Future work will involve implementing the exercise and testing it with a real-life exoskeleton, as presented, as well as developing intelligent-algorithm-based controllers that predict motion progression and respond by adjusting support in nearly real-time.

References

1. Bibrowicz, K., Ogrodzka-Ciechanowicz, K., Hudakova, Z., Szurmik, T., Bibrowicz, B., Kurzeja, P.: Pelvic asymmetry and stiffness of the muscles stabilizing the lumbo–pelvic–hip complex (lphc) in tensiomyography examination. Journal of Clinical Medicine **14**(7), 2229 (2025)
2. Dehcheshmeh, F.G., Nourbakhsh, M.R., Shafizadegan, Z., Farsani, Z.A., Arab, A.M.: Pelvic and lower limb kinematics in individuals with chronic low back pain during sit-to-stand function: A cross-sectional study. Journal of Manipulative and Physiological Therapeutics **47**(1-4), 85–95 (2024)
3. Falkowski, P., Oleksiuk, J., Jeznach, K., Aktan, M.E.: Method of automatic biomedical signals interpretation for safety supervision and optimisation of the exoskeleton-aided physiotherapy of lower extremity. In: Proceedings of the 2024 4th International Conference on Robotics and Control Engineering, pp. 57–63 (2024)
4. Falkowski, P., Pikuliński, M., Osiak, T., Jeznach, K., Zawalski, K., Kołodziejski, P., Zakręcki, A., Oleksiuk, J., Śliż, D., Osiak, N.: Similarity analysis of upper extremitys trajectories in activities of daily living for use in an intelligent control system of a rehabilitation exoskeleton. In: Actuators, vol. 14, p. 324. MDPI (2025)
5. Falkowski, P., Zawalski, K., Oleksiuk, J., Leczkowski, B., Pilat, Z., Aktan, M.E., Akdogan, E., Niedbalski, P., Ömürlü, V.E., Jarek, M., et al.: Systematic review of mechanical designs of rehabilitation exoskeletons for lower-extremity. Archive of Mechanical Engineering **71** (2024)
6. Hasan, S., Dhingra, A.K.: Biomechanical design and control of an eight dof human lower extremity rehabilitation exoskeleton robot. Results in Control and Optimization **7**, 100,107 (2022)
7. Kirk, B., French, C., Gebauer, M., Vogrin, S., Zanker, J., Sales, M., Duque, G.: Diagnostic power of relative sit-to-stand muscle power, grip strength, and gait speed

for identifying a history of recurrent falls and fractures in older adults. European geriatric medicine **14**(3), 421–428 (2023)
8. Lau, J.C., Mombaur, K.: Can lower-limb exoskeletons support sit-to-stand motions in frail elderly without crutches? a study combining optimal control and motion capture. Frontiers in Neurorobotics **18**, 1348,029 (2024)
9. Lin, W., Xiong, Y., Zhang, C., Wang, X., Han, B.: Research and design of a medial-support exoskeleton chair. Biomimetics **10**(5), 330 (2025)
10. Ratnakumar, N., Akbaş, K., Jones, R., You, Z., Zhou, X.: Predicting sit-to-stand motions with a deep reinforcement learning based controller under idealized exoskeleton assistance. Multibody System Dynamics pp. 1–18 (2024)
11. Rosales-Luengas, Y., Espinosa-Espejel, K.I., Lopéz-Gutiérrez, R., Salazar, S., Lozano, R.: Lower limb exoskeleton for rehabilitation with flexible joints and movement routines commanded by electromyography and baropodometry sensors. Sensors **23**(11), 5252 (2023)
12. Yang, C., Zhang, X., Zhang, L., Zou, C., Peng, Z., Huang, R., Cheng, H.: Coordinated energy-efficient walking assistance for paraplegic patients by using the exoskeleton-walker system. OAE Publishing Inc. (2024)
13. Yu, S., Liu, C., Ye, C., Fu, R.: Passive and active training control of an omnidirectional mobile exoskeleton robot for lower limb rehabilitation. In: Actuators, vol. 13, p. 202. MDPI (2024)
14. Zhou, J., Yang, S., Xue, Q.: Lower limb rehabilitation exoskeleton robot: A review. Advances in Mechanical Engineering **13**(4), 16878140211011,862 (2021)